International Journal of Applied Engineering Research ISSN 0973-4562 Volume 13, Number 6 (2018) pp. 3524-3532

Adaptive Super-Twisting Sliding Mode Control for Wind Energy Conversion System

Saïd Boubzizi[1,2], Hafedh Abid[1], Ahmed El hajjaji[2], Mohamed Chaabane[1]

[1] Lab-STA Laboratory, National Engineering School of Sfax, University of Sfax, Route de la Soukra 3029 Sfax, Tunisia.
[2] MIS Laboratory, University of Picardie Jules Verne, 33, Rue Saint-Leu, 80039 Amiens, France.

Abstract

This paper deals with control strategy of a Wind Energy Conversion System (WECS) equipped with Doubly-Fed-Induction-Generator (DFIG). The novelty of this controller concerns the Adaptive-Super-Twisting (ASTW) based design algorithm for the DFIG control. The proposed controller ensures free-chattering response, finite-time-convergence and improves accuracy without needing time derivative of its sliding surface. An interesting point comes from the proposed adaptive gain strategy which permits to reduce by 50% the number of gains to be adapted which is interesting for systems with several controllers such as WECS (Turbine + generator + grid). The stability analysis of the proposed control is proved using the Lyapunov candidate function approach. The designed ASTW algorithm has been compared to conventional STW-SMC and tested using 1.5MW -wind turbine simulator FAST (Fatigue, Aerodynamics, Structures, and Turbulence) which is developed by the National Renewable Energy Laboratory (NREL), USA.

Keywords: Wind turbine (WT), Doubly-fed_induction generator (DFIG), Power generation, ASTW (Adaptive_Super twisting), Sliding mode control (SMC)

INTRODUCTION

Wind power has been one of the world's leading renewable energy suppliers in the last years. This source of power generation which produces clean energy plays a more important role in the way our world is powered, as it can also solve the problem of importing energy around the world and meet the energy needs of isolated sites. By the end of 2016, global wind installed capacity was 486.7 GW which represents an increase of 12% market growth from the number in 2015, mainly in china 145.3 MW, United States 74.48 MW, Germany 44.947 MW, India 25 MW, Spain 23 MW, United Kingdom 13 MW, Canada 11.2 MW, and France 10,4 MW [1]. This growth is due to the astonishing increase of global new installations 63,467 MW in 2015 which represents a growth of 22% of the annual market [1].

Variable-speed-wind-turbine (VSWT) and double fed induction generator have been taking increasing attention during the last decades, since they can work in a wide range of wind speed and have four-quadrant-power capabilities. Furthermore, wind turbine (WT) based on double fed induction generator (DFIG) has the advantage of reducing converter prices to only 25% of the nominal power, which contributes considerably to reduce costs.

To effectively extract wind power, the tip-speed-ratio of the WT should be maintained at its optimum despite wind-speed variations. However, the mechanical and electrical parts of wind energy conversion system (WECS) work generally as a nonlinear-system where parametric variations and unmodeled-dynamics are the major problems which could deviate the system from its optimal operation. In addition, VSWTs are expected to work under high wind-speed variations, making their control design a serious challenge, particularly, with large wind turbines. In this context, several research studies have been developed to improve the control strategies for the WT-DFIG system. Field-Oriented-Control using Proportional–Integral (PI) controllers is one of the famous methods due to its simple design [2]. However, this control scheme may have low performance under medium and high wind speed variation because of its sensitivity to system parameters and external disturbances. Therefore, to overcome these drawbacks further nonlinear-control techniques have been used, such as fuzzy logic control [3], [4], predictive control [5] and neural networks control [6]. Sliding-mode approach is an effective solution for controlling perturbed-systems [7]. Although Sliding mode control (SMC) is robust, insensitive to external perturbations and uncertainties of the system, it unfortunately generates undesirable chattering [7]. High order sliding mode control (HOSMC) techniques are among the appropriate alternatives for avoiding chattering effects [8], [9], [10]. This approach ensures driving of sliding surface and its successive derivatives to zero as well as increases the stabilization of the system. Super-Twisting (STW) algorithm is a second-order SMC. The idea consists in generating a continuous control function which ensures the convergence of the variable surface and its derivative in finite time under a gradient of delimited perturbations, at a known limit. Indeed, standard STW algorithm includes a discontinuous term under its integral, so the chattering is attenuated but not removed. This standard control requires knowledge of the limits of the disturbance gradients which is not an easy task in practical cases. This results in an overestimation of the disturbance limit while developing the STW laws which leads to higher control gains. The main contribution of this paper, which deals with WT-DFIG is the control approach, which is original due to the proposed adaptive algorithm system that permits not only an online adaptation of control gains but also, reduces by 50% number of gains to be adjusted compared to strategy proposed by [11]. The proposed strategy is interesting for systems with

several controllers such as WT-DFIG system (Turbine + generator + grid). The controller is fully based on an Adaptive Super Twisting control (ASTW) that ensures the convergence of the sliding surface to zero without over-estimating the algorithm gains with unknown bounded uncertainties / perturbations.

This paper is organized as follows section 2 describes the wind energy conversion system based on DFIG. Section 3 presents the proposed control strategy of the DFIG. Finally, section 4 gives simulated results of the proposed controller.

DESCRIPTION OF WECS

This note focuses on one of the most popular configurations in wind energy conversion systems with a fixed pitch and variable speed wind turbine. A comprehensive scheme of WT-DFIG structure is shown in figure 1.

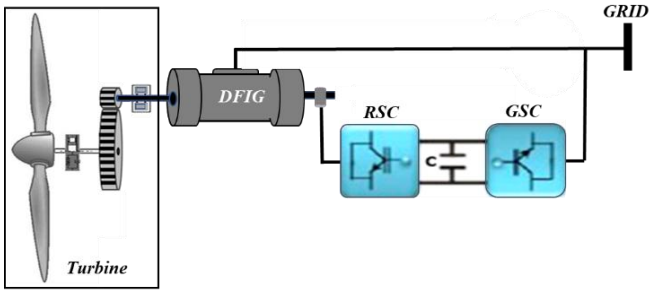

Figure 1. WECS based on DFIG

The expression of aerodynamic power extracted from the wind is given by, [12]

$$P_a = \frac{1}{2}\pi R^2 \rho C_p(\lambda) v^3 \tag{1}$$

where R, C_p, v and ρ denote consecutively the radius and the power coefficient of the WT, the wind speed and the air density.

The tip-speed-ratio is defined as

$$\lambda = \frac{R\omega_r}{v} \tag{2}$$

The power extraction of a wind turbine is a function of the available wind power, the power curve of the machine and the ability of the machine to respond to wind fluctuation as shown in figure 2 and figure 4.

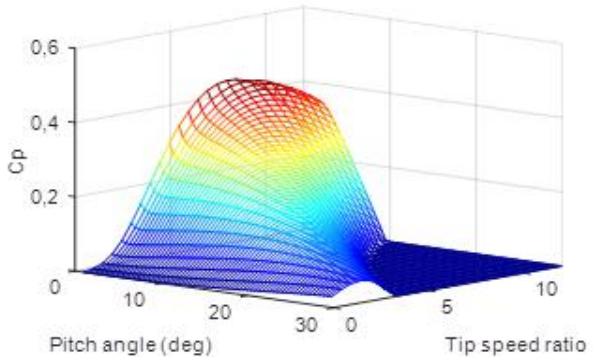

Figure 2. WT power coefficient

The slow angular velocity of the turbine ω_r is adapted to the fast speed of the generator ω by the following relation

$$n_g = \frac{\omega}{\omega_r} \tag{3}$$

The global mechanical dynamics of the rotor can be expressed as follows, [13]

$$J\dot{\omega}_r = T_a - K\omega_r - T_g + \kappa \tag{4}$$

with $\begin{cases} J = J_r + n_g^2 J_g \\ K = K_r + n_g^2 K_g \\ T_g = n_g T_{em} \end{cases}$

κ denotes the unmodeled dynamics and external disturbances.

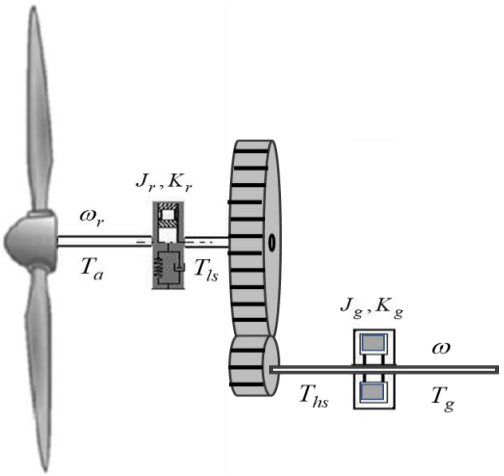

Figure 3. Wind turbine drive-train

To achieve maximum efficiency, rotor speed should track the reference given by the Maximum Power Point Tracking (MPPT), under different wind speed patterns.

$$T_{ref} = k_{opt}\omega_r^2, \quad k_{opt} = \frac{1}{2}\pi\rho R^5 \frac{C_{p\max}}{\lambda_{opt}^3}, \quad \omega_{ref} = \lambda_{opt}\frac{v}{R} \tag{5}$$

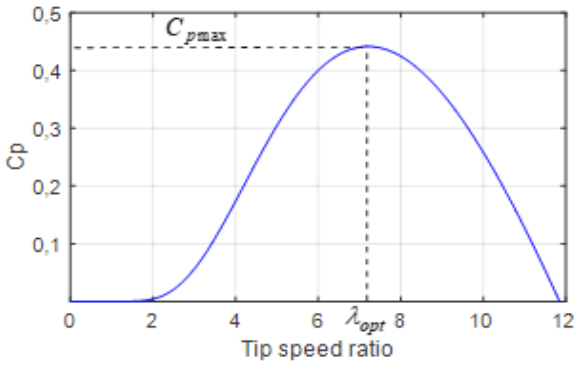

Figure 4. C_p–λ characteristics

The dynamic model of the DFIG is described in a synchronously rotating frame d-q, [14]

$$\begin{cases} V_{sd} = R_s I_{sd} + \dot{\phi}_{sd} - \omega_s \phi_{sq} \\ V_{sq} = R_s I_{sq} + \dot{\phi}_{sq} + \omega_s \phi_{sd} \end{cases}, \begin{cases} V_{rd} = R_r I_{rd} + \dot{\phi}_{rd} - \omega \phi_{rq} \\ V_{rq} = R_r I_{rq} + \dot{\phi}_{rq} + \omega \phi_{rd} \end{cases} \quad (6)$$

where ω_s is synchronous speed.

The flux linkages are given by

$$\begin{cases} \phi_{sd} = L_s I_{sd} + M I_{rd} \\ \phi_{sq} = L_s I_{sq} + M I_{rq} \end{cases}, \begin{cases} \phi_{rd} = L_r I_{rd} + M I_{sd} \\ \phi_{rq} = L_r I_{rq} + M I_{sq} \end{cases} \quad (7)$$

The electromagnetic torque, the active and the reactive power generated by the generator can be expressed as follows [10]

$$\begin{cases} P = V_{sd} I_{sd} + V_{sq} I_{sq} \\ Q = V_{sq} I_{sd} - V_{sd} I_{sq} \end{cases}, \quad T_{em} = n_p \frac{M}{L_s} \left(I_{rd} \phi_{sq} - I_{rq} \phi_{sd} \right) \quad (8)$$

By applying the following vector alignment [10], we obtain

$$\begin{cases} \phi_{sd} = \phi_s \\ \phi_{sq} = 0 \end{cases}, \begin{cases} V_{sd} = 0 \\ V_s = V_{sq} = \omega_s \phi_{sd} \end{cases} \quad (9)$$

and

$$\begin{cases} \dot{I}_{rd} = \frac{1}{\sigma L_r} \left(V_{rd} - R_r I_{rd} + s \omega_s \sigma L_r I_{rq} - \frac{M}{L_s} \dot{\phi}_s \right) \\ \dot{I}_{rq} = \frac{1}{\sigma L_r} \left(V_{rq} - R_r I_{rq} - s \omega_s \sigma L_r I_{rd} - s \omega_s \frac{M}{L_s} \phi_s \right) \end{cases} \quad (10)$$

where, $\sigma = 1 - \frac{M^2}{L_s L_r}$, n_p is the pole pair number and s is the slip speed.

Hence, the electromagnetic torque becomes

$$T_{em} = k_e I_{rq} \quad \text{with} \quad k_e = -n_p \frac{M}{L_s} \phi_s \quad (11)$$

CONTROL OF THE DFIG

The control of WT-DFIG must be a compromise between maintaining the optimum performance and limiting the oscillations of torque. This results in maximum power extraction.

Based on relation (9), the stator-side reactive power of the DFIG given by (8) can be written as follows

$$Q = \frac{V_s}{L_s} \left(\phi_s - M I_{dr} \right) \quad (12)$$

By setting equation (12) to zero, the rotor reference current $I_{rd,ref}$ is obtained as

$$I_{rd,ref} = \frac{\phi_s}{M} = \frac{V_s}{\omega_s M} \quad (13)$$

The main objectives in this work, is to maximize wind power generation by reaching optimal torque T_{ref}, ensuring zero reactive power and improving quality of the generated energy. Those objectives can be successfully fulfilled through a robust control strategy.

Let's consider the following tracking errors of rotor current and electromagnetic torque

$$S = \begin{cases} S_1 = I_{rd} - I_{rd\_ref} \\ S_2 = T_{em} - T_{ref} \end{cases} \quad (14)$$

Systems of equations (6) can be described by the following block diagram figure 5.

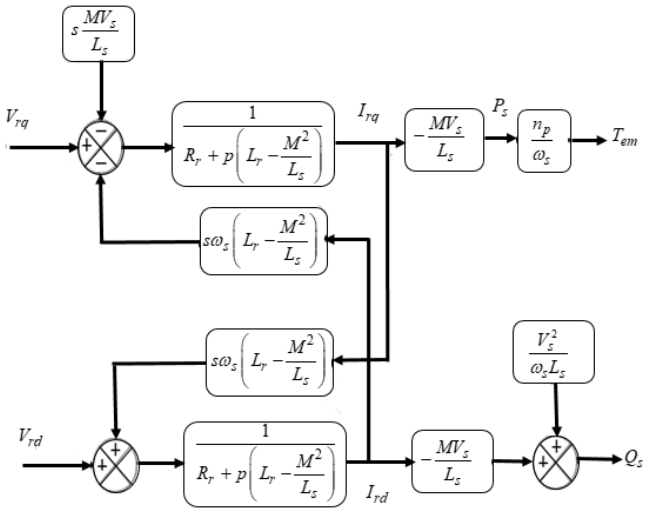

Figure 5. System to be controlled

- *Adaptive Super-Twisting sliding mode control*

High order sliding mode control is an effective method to overcome the chattering problem. In fact, a control order *"n"* acts on *"n"* derivatives. This feature helps to attenuate the undesirable chattering while preserving the prosperity of the robustness of the SMC approach [15]. However, the implementation of an *n-th* order controller requires knowledge of the *n-th* consecutive sliding surfaces. The exception is the STW algorithm which needs only information on the sliding surface S ,[16]. In the following, an adaptive Super_Twisting

(ASTW) control strategy is proposed to improve the performance and effectiveness of the WT-DFIG system.

The derivative of system (14) is

$$\begin{cases} \dot{S}_1 = \dfrac{1}{\sigma L_r}\left(V_{rd} - R_r I_{rd} + s\omega_s \sigma L_r I_{rq} - \dfrac{M}{L_s}\dot{\phi}_s\right) - \dot{I}_{rd-ref} \\ \dot{S}_2 = -n_p \dfrac{M}{\sigma L_s L_r}\phi_s\left(V_{rq} - R_r I_{rq} - s\omega_s \sigma L_r I_{rd} - s\omega_s \dfrac{M}{L_s}\phi_s\right) - \dot{T}_{ref} \end{cases} \quad (15)$$

Let's consider functions G_1 and G_2 as follows:

$$\begin{cases} G_1 = \dfrac{1}{\sigma L_r}\left(-R_r I_{rd} + s\omega_s L_r \sigma I_{rq} - \dfrac{M}{L_s}\dot{\phi}_s\right) - \dot{I}_{rd\_ref} \\ G_2 = -n_p \dfrac{M}{\sigma L_s L_r}\phi_s\left(-R_r I_{rq} - s\omega_s L_r \sigma I_{rd} - s\omega_s \dfrac{M}{L_s}\phi_s\right) - \dot{T}_{ref} \end{cases} \quad (16)$$

Assumption 1: We assume that functions G_1, G_2 are bounded $|G_1| \le \delta_1 |S_1|^{1/2}$, $|G_2| \le \delta_2 |S_2|^{1/2}$
where δ_1, δ_2 are positive unknown constants.

Then, equation (15) can be written as:

$$\begin{cases} \dot{S}_1 = \dfrac{1}{\sigma L_r} V_{rd} + G_1 \\ \dot{S}_2 = -n_p \dfrac{M}{\sigma L_s L_r}\phi_s V_{rq} + G_2 \end{cases} \quad (17)$$

The control laws are given by:

$$\begin{cases} V_{rd} = y_1 - a_1(S_1,t)|S_1|^{1/2}\,\mathrm{sgn}(S_1) \\ \dot{y}_1 = -b_1(S_1,t)\,\mathrm{sgn}(S_1) \\ V_{rq} = y_2 + a_2(S_2,t)|S_2|^{1/2}\,\mathrm{sgn}(S_2) \\ \dot{y}_2 = +b_2(S_2,t)\,\mathrm{sgn}(S_2) \end{cases} \quad (18)$$

where, the adaptive gains are

$$\begin{cases} a_i(S_i, \dot{S}_i, t), \\ b_i(S_i, \dot{S}_i, t) \end{cases} \text{ for } i = 1,2 \quad (19)$$

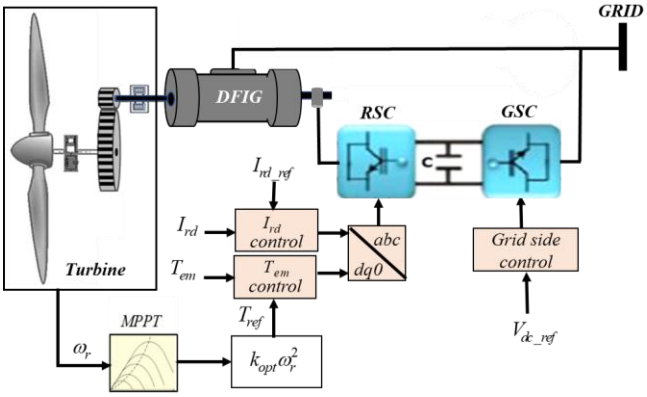

Figure 6. Block-scheme of the proposed WT-DFIG control strategy

V_{rd} controls the reactive power (I_{rd}) and V_{rq} controls the active power (T_{em}).

Assumption 1. We assume that G_1 and G_2 are bounded functions which satisfy the following conditions: $|G_1(t,S_1)| < \delta_1 |S_1|^{1/2}$ and $|G_2(t,S_2)| < \delta_2 |S_2|^{1/2}$, where δ_1 and δ_2 are some positive constants.

The theorem below which is inspired from [17], provides sufficient conditions to ensure the stability and robustness of current and electromagnetic torque control of the DFIG.

Theorem 1: Consider the system described by equation (10) and the sliding surface given by (14). If we apply the control law (18) based on Second Order Sliding Mode Controller to the system. The closed-loop system (15) is ensured with finite-time convergence with the following adaptive gains $(a_i, b_i$ for $i = 1,2)$

$$\begin{cases} \dot{a}_i(t,S_i) = \begin{cases} k_i\sqrt{\dfrac{\gamma_i}{2}}\,\mathrm{sign}(S_i), & \text{if } |S_i| > \mu_i \\ 0, & \text{if } |S_i| \le \mu_i \end{cases} \\ b_i(t,S_i) = 2\varepsilon_i a_i(t,S_i) + \lambda_i + 4\varepsilon_i^2 \end{cases} \quad (20)$$

where $\varepsilon_i, k_i, \lambda_i, \mu_i$ and γ_i are arbitrary positive constants. The parameter μ_i is introduced in order to get only positive values for $a_i(t,S_i) > 0$.

Proof of convergence

Let us consider the case of V_{rd}

$$\dot{S}_1 = \frac{1}{\sigma L_r} V_{rd} + G_1 \quad (22)$$

and

$$\begin{cases} \dot{S}_1 = -qa_1|S_1|^{1/2}\,\mathrm{sgn}(S_1) + \omega_* + G_1 \\ \dot{\omega}_* = -qb_1\,\mathrm{sgn}(S_1) \end{cases} \quad (23)$$
$$q = \frac{1}{\sigma L_r}, \omega_* = qy_1$$

where $a_1(t,S_1)$ and $b_1(t,S_1)$ are adaptive gains:

$$\begin{cases} \dot{a}_1(t,S_1) = \begin{cases} k_1\sqrt{\dfrac{\gamma_1}{2}}\,\mathrm{sign}(S_1), & \text{if } |S_1| > \mu_1 \\ 0, & \text{if } |S_1| \le \mu_1 \end{cases} \\ b_1(t,S_1) = 2\varepsilon_1 a_1(t,S_1) + \lambda_1 + 4\varepsilon_1^2 \end{cases} \quad (24)$$

Let's introduce the following new vector:

$$z = (z_1, z_2)^T = \left(|S_1|^{1/2}\,sgn(S_1), \omega_*\right)^T \quad (25)$$

We can easily deduce the derivative of (25)

$$\begin{cases} \dot{z}_1 = \dfrac{1}{|z_1|}\left(-\dfrac{qa_1}{2}z_1 + \dfrac{1}{2}z_2 + \dfrac{1}{2}G_1\right) \\ \dot{z}_2 = -\dfrac{qb_1}{|z_1|}z_1 \end{cases} \tag{26}$$

Using assumption A1, we get

$$G_1(x,t) = \rho_1(x,t)|S_1|^{1/2}\,\mathrm{sgn}(S_1) = \rho_1(x,t)z_1 \tag{27}$$

where $\rho_1(x,t)$ is a bounded function, $0 < \rho_1(x,t) < \delta_1$:

$$\dot{z} = A(z_1, z_2)z \tag{28}$$

with

$$A(z_1, z_2) = \frac{1}{2|z_1|}\begin{bmatrix} -qa_1 + \rho_1 & 1 \\ -qb_1 & 0 \end{bmatrix} \tag{29}$$

The stability analysis of (28), can be proved using Lyapunov candidate function (30), inspired from [17]

$$V(z, a_1, b_1)^T = V_0 + \frac{1}{2\gamma_1}\left(a_1 - a_1^*\right)^2 + \frac{1}{2\bar{\gamma}_1}\left(b_1 - b_1^*\right)^2 \tag{30}$$

where

$$V_0(z) = \left(\lambda_1 + 4\varepsilon_1^2\right)z_1^2 + z_2^2 - 4\varepsilon z_1 z_2 = z^T P z \tag{31}$$

$$P = \begin{bmatrix} \lambda_1 + 4\varepsilon_1^2 & -2\varepsilon_1 \\ -2\varepsilon_1 & 1 \end{bmatrix}$$

where P is a positive definite matrix $\lambda_1 > 0$, $\bar{\gamma}_1 > 0$, $|a_1(t, S_1)| \le a_1^*$ and $|b_1(t, S_1)| \le b_1^*$, $\forall t \ge 0$.

Hence, the derivative of (30)

$$\dot{V}(z, a_1, b_1)^T = z^T\left[A^T P + PA\right]z + \frac{1}{\gamma_1}\varepsilon_{a1}\dot{a}_1 + \frac{1}{\bar{\gamma}_1}\varepsilon_{b1}\dot{b}_1 \tag{32}$$

where $\varepsilon_{a1} = a_1 - a_1^*$ and $\varepsilon_{b1} = b_1 - b_1^*$.

The first term of equation (32)

$$\dot{V}_0(z, a_1, b_1)^T = z^T\left[A^T P + PA\right]z \le -\frac{1}{2|z_1|}z^T Q z \tag{33}$$

where

$$Q = \begin{bmatrix} Q_{11} & Q_{12} \\ Q_{21} & 4\varepsilon \end{bmatrix}$$

with $\begin{cases} Q_{11} = 2\lambda_1 q a_1 + 4q\varepsilon_1(2\varepsilon_1 a_1 - b_1) - 2\rho_1\left(\lambda_1 + 4\varepsilon_1^2\right). \\ Q_{12} = Q_{21} = \left(qb_1 - 2q\varepsilon_1 a_1 - \lambda_1 - 4\varepsilon_1^2\right) + 2\varepsilon_1\rho_1. \end{cases}$

By choosing

$$b_1 = 2\varepsilon_1 a_1 + \lambda_1 + 4\varepsilon_1^2 \tag{34}$$

Then, Q will be positive definite matrix if a_1 is large enough satisfying:

$$a_1 > \frac{\sigma L_r \delta_1\left(\lambda_1 + 4\varepsilon_1^2\right) + 2\varepsilon_1\left(\lambda_1 + \varepsilon_1^2\right)}{\lambda_1} \tag{35}$$

From (33), we have

$$\dot{V}_0(z) \le -\frac{1}{2|z_1|}z^T Q z \le -\frac{2\varepsilon_1}{2|z_1|}z^T z = -\frac{\varepsilon_1}{|z_1|}\|z\|^2 \tag{36}$$

We note $\lambda_{\min}(P)$ and $\lambda_{\max}(P)$ as the minimal and maximal eigenvalues of matrix P, then we can write:

$$\lambda_{\min}(P)\|z\|^2 \le z^T P z \le \lambda_{\max}(P)\|z\|^2$$

In view of (25), we deduce

$$\|z\|^2 = z_1^2 + z_2^2 = |S_1| + z_2^2$$

and $|z_1| = |S_1|^{1/2} \le \|z\| \le \dfrac{V_0^{1/2}(z)}{\lambda_{\min}^{1/2}(P)}$

Then, we can conclude

$$\dot{V}_0(z) \le -rV_0^{1/2} \tag{37}$$

where, $r = \dfrac{\varepsilon\lambda_{\min}^{1/2}(P)}{\lambda_{\max}(P)}$

Incorporating with (32) and (37), we obtain

$$\begin{aligned} \dot{V} \le -rV_0^{1/2} - \frac{k_1}{\sqrt{2\gamma_1}}|\varepsilon_{a1}||S_1| - \frac{\bar{k}_1}{\sqrt{2\bar{\gamma}_1}}|\varepsilon_{b1}||S_1| + \frac{1}{\gamma_1}\varepsilon_{a1}\dot{a}_1 \\ + \frac{1}{\bar{\gamma}_1}\varepsilon_{b1}\dot{b}_1 + \frac{k_1}{\sqrt{2\gamma_1}}|\varepsilon_{a1}||S_1| + \frac{\bar{k}_1}{\sqrt{2\bar{\gamma}_1}}|\varepsilon_{b1}||S_1| \end{aligned} \tag{38}$$

Consider the well-known inequality

$$\left(x^2 + y^2 + z^2\right)^{1/2} \le |x| + |y| + |z|$$

and in view of (38), we can derive

$$\begin{aligned} &-rV_0^{1/2} - \frac{k_1}{\sqrt{2\gamma_1}}|\varepsilon_{a1}||S_1| - \frac{\bar{k}_1}{\sqrt{2\bar{\gamma}_1}}|\varepsilon_{b1}||S_1| \\ &\le -\eta_1\left(V_0 + \frac{1}{2\gamma_1}(\varepsilon_{a1}S_1)^2 + \frac{1}{2\bar{\gamma}_1}(\varepsilon_{b1}S_1)^2\right)^{1/2} \end{aligned} \tag{39}$$

with $\eta_1 = \min\left(r, k_1, \bar{k}_1\right)$

Let's note term V_1 as follows

$$V_1 = V_0 + \frac{1}{2\gamma_1}(\varepsilon_{a1}S_1)^2 + \frac{1}{2\bar{\gamma}_1}(\varepsilon_{b1}S_1)^2$$

From (39), we can rewrite (38) as

$$\dot{V}(z,a_1,b_1) \le -\eta_1 V_1^{1/2} + \frac{1}{\gamma_1}\varepsilon_{a1}\dot{a}_1 + \frac{1}{\bar{\gamma}_1}\varepsilon_{b1}\dot{b}_1 + \frac{k_1}{\sqrt{2\gamma_1}}|\varepsilon_{a1}S_1| + \frac{\bar{k}_1}{\sqrt{2\bar{\gamma}_1}}|\varepsilon_{b1}S_1| \quad (40)$$

Now we assume that adaptation adaptive gains $a_1(t)$ and $b_1(t)$ are bounded such that $|a_1(t)| \le a_1^*$ and $|b_1(t)| \le b_1^*$, $\forall t \ge 0$, then (40) becomes

$$\dot{V}(z,a_1,b_1) \le -\eta_1 V_1^{1/2} - |\varepsilon_{a1}|\left(\frac{1}{\gamma_1}\dot{a}_1 - \frac{k_1}{\sqrt{2\gamma_1}}|S_1|\right) - |\varepsilon_{b1}|\left(\frac{1}{\bar{\gamma}_1}\dot{b}_1 - \frac{\bar{k}_1}{\sqrt{2\bar{\gamma}_1}}|S_1|\right) \quad (41)$$

Thus, we obtain

$$\dot{V}(z,a_1,b_1) \le -\eta_1 V_1(z,a_1,b_1)^{1/2} + \xi \quad (42)$$

where

$$\xi = -|\varepsilon_{a1}|\left(\frac{1}{\gamma_1}\dot{a}_1 - \frac{k_1}{\sqrt{2\gamma_1}}|S_1|\right) - |\varepsilon_{b1}|\left(\frac{1}{\bar{\gamma}_1}\dot{b}_1 - \frac{\bar{k}_1}{\sqrt{2\bar{\gamma}_1}}|S_1|\right)$$

By choosing $\xi = 0$, we can ensure the finite time convergence through the following dynamic adaptation gains

$$\dot{a}_1 = k_1\sqrt{\frac{\gamma_1}{2}}|S_1| \quad (43)$$

From adaptation law (24) and (43), we have

$$b_1 = 2\varepsilon_1 a_1 + \lambda_1 + 4\varepsilon_1^2 \rightarrow \dot{b}_1 = 2\varepsilon_1\dot{a}_1 = \bar{k}_1\sqrt{\frac{\bar{\gamma}_1}{2}}|S_1|$$

By selecting $\varepsilon_1 = \frac{\bar{k}_1}{2k_1}\sqrt{\frac{\bar{\gamma}_1}{\gamma_1}}$, we ensure that $\xi = 0$.

Hence, the derivative of system (30) is guaranteed definite negative and thus convergence of $S_1 = 0$ which can be finally written as follows:

$$\dot{V}(z,a_1,b_1) \le -\eta_1 V_1^{1/2} \quad (45)$$

with $\eta_1 > 0$.

Similar development can be used to prove the stability analysis in the case of V_{rq}.

- ***Simulation using FAST Code simulator***

The proposed Adaptive Super-Twisting algorithm has been tested for validation using FAST (Fatigue-Aerodynamics-Structures-Turbulence) software which is an effective aero-elastic simulator that can predict extreme and fatigue loads of a spread of WT's configurations (two and three-blade horizontal-axis) [18]. FAST relies on advanced engineering models derived from basic laws with appropriate assumptions. This simulator is validated by the German company Germanischer-Lloyd-WindEnergie, which specializes in certification and testing of WT's. FAST have many input for turbine control settings, environmental conditions, blade models,etc, to help researchers evaluate wind energy offshore technology figure 7.

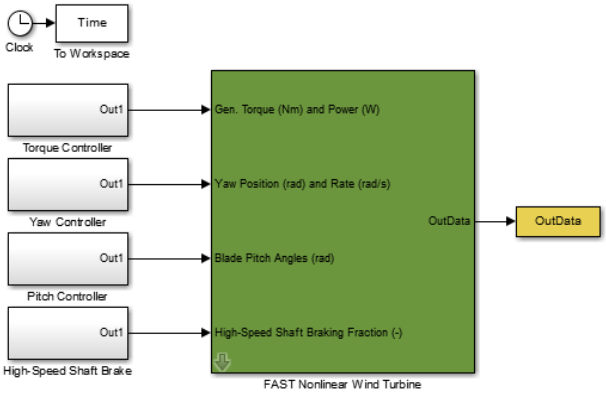

Figure 7. FAST wind turbine model in Simulink

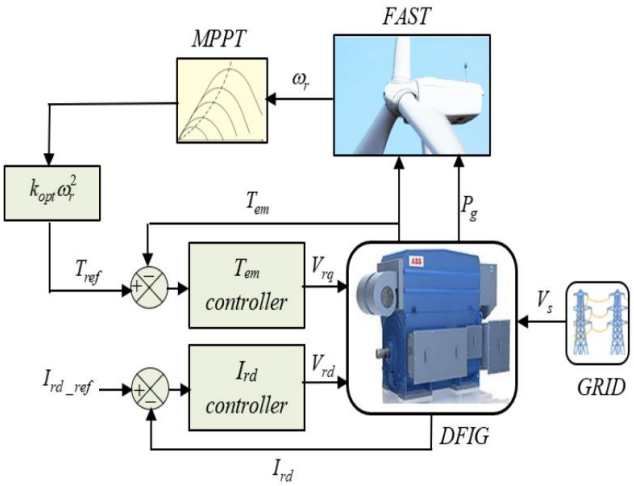

Figure 8. Block diagram of the global system

SIMULATION RESULTS AND DISCUSSION

The proposed control strategy has been validated with numerical validation using 1.5 MW 3-blade-WT FAST simulator, developed by National Renewable Energy Laboratory (NREL), figure 8.

The wind inflow for the simulation generated by FAST simulator is shown in figure 9. The wind speed profile represents a turbulent wind speed variation between 8 m/s and 14.5 m/s. Figure 10 shows the mechanical speed of the generator until 1800 rpm. The desired DFIG reference are directly tracked through an Adaptive Super-Twisting control. As can be clearly seen in figure 11 and figure 14, the electromagnetic torque and rotor current of the DFIG show good tracking performances under turbulent wind-speed variation. The rotor current reference in figure 11 is determined as a function of stator voltage V_s. Figure 14 represents the

electromagnetic torque response and the aerodynamic torque of the simulator, its maximum value is around -8.4 KN.m. The proposed ASTW control strategy does not induce increased mechanical stress and ensures smooth aerodynamic torque variations. The simulation results displayed in figure 12 and figure 13 show that the gains $a_1(S_1,t)$ and $a_2(S_2,t)$ are growing quickly as the disturbances are quicker eliminated, which permits faster convergence of sliding surface to zero. $b_1(S_1,t)$ and $b_2(S_2,t)$ are deduced from $a_1(S_1,t)$ and $a_2(S_2,t)$ according to the proposed adaptation laws. Figures 9-15 prove the efficiency of the proposed ASTW control algorithm in terms of tracking error, free chattering and better power quality generation figure 15 compared to standard super-twisting SMC with fixed gains presented in figure 16. The proposed control overcomes the problem of undesirable chattering of standard control while ensuring the robustness features of SMC.

The presented results show that a standard SOSMC control method can be an interesting solution for systems based DFIG technology for wind power conversion. However, chattering effect remains a significant problem with this technique. The results obtained show that ASTW strategy effectiveness is more attractive in terms of power energy quality and higher accuracy. The proposed control strategy reduced the number of gains to be adjusted via an adaptation algorithm.

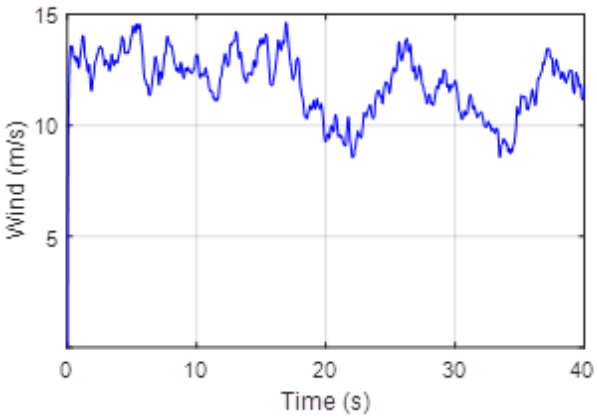

Figure 9. Wind speed profile (m/s)

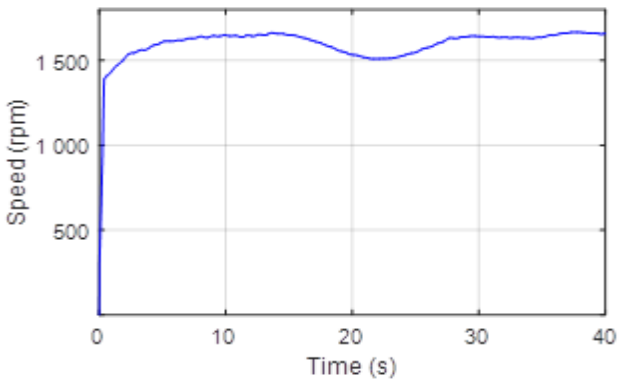

Figure 10. DFIG mechanical speed.

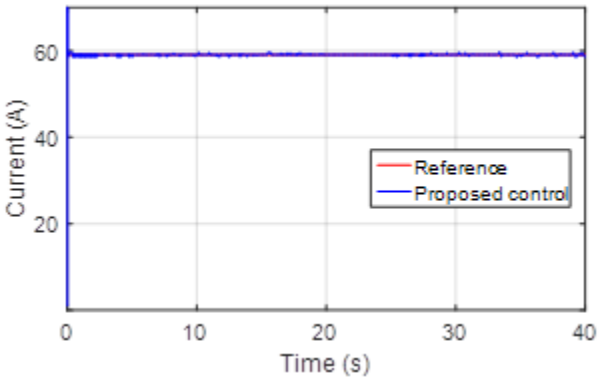

Figure 11. Current I_{rd} tracking.

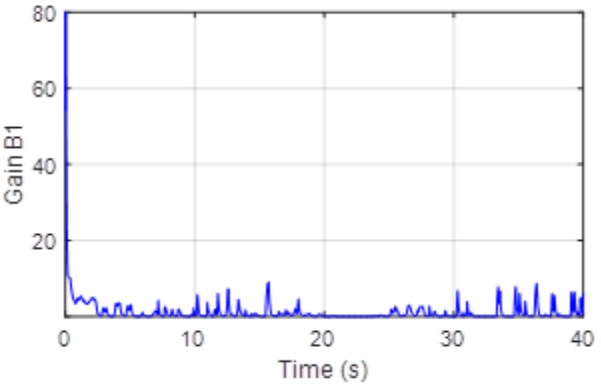

Figure 12. Gain adaptation B_1.

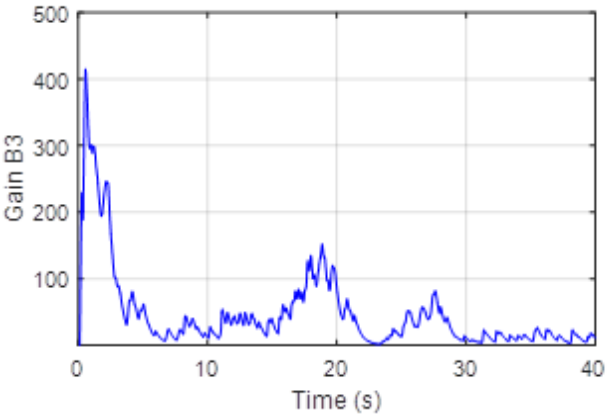

Figure 13. Gain adaptation B_3.

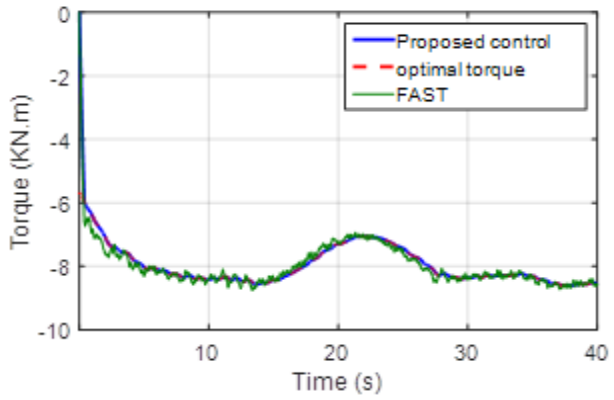

Figure 14. Electromagnetic torque.

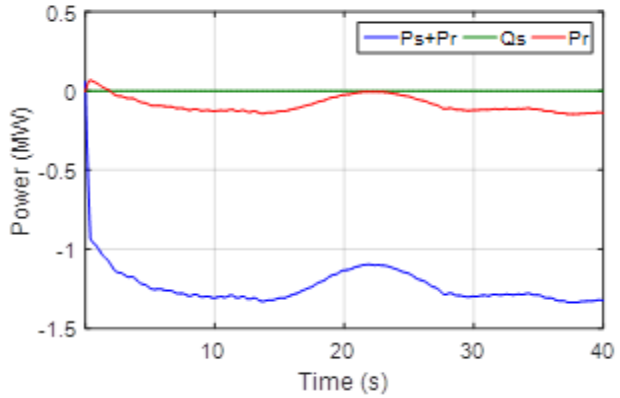

Figure 15. Active power (MW), reactive power (MVar) with proposed control.

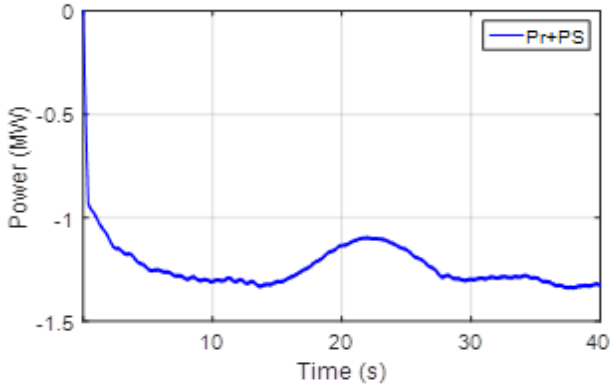

Figure 16. Active power with the standard control.

CONCLUSION

An Adaptive-Super-Twisting algorithm based on SMC control strategy is developed for wind energy conversion system. The proposed Lyapunov-based second order sliding mode approach allows an online adaptation of control gains and ensures the convergence in a finite-time. The boosted, robustness and stability of the proposed control strategy have been compared to conventional STW-SMC under FAST wind turbine emulator. The obtained results with ASTW are more significant and satisfactory in terms of power extraction maximization, higher accuracy, faster convergence, free chattering, no overflow and without induced mechanical stress which contributes to increase reliability and improve the system's energy efficiency.

Table 1. Wind Turbine and DFIG Parameters

Turbine diameter (m)	$D = 70$
Air-density (kg.m3)	$\rho = 1.225$
Gear reduction ratio	$n_g = 75$
Stator-resistance (Ω)	$R_s = 0.00297$
Rotor-resistance (Ω)	$R_r = 0.00382$
Stator-inductance (H)	$L_s = 0.121$
Rotor-inductance (H)	$L_r = 0.0573$
Cyclic-inductance (H)	$M = 0.031$
Number of pole pairs	$n_p = 2$

Table 2. ASTW Control Parameters

k_1	k_2	γ_1	γ_2	$\varepsilon_1 = \varepsilon_2$
80	100	1	12	4

REFERENCES

[1] Global Wind Energy Council Statistics, GWEC, www.gwec.net/global-figures/graphs/, 2017.

[2] Saurabh, M., Amar, N., Deependra, S., 2016, "Optimum design of Proportional-Integral controllers in grid-integrated PMSG-based wind energy conversion system," International Transactions on Electrical Energy Systems, 26, pp. 1006-1031.

[3] Mohamed, A., Eskander, M., Ghali, F., 2001, "Fuzzy logic control based maximum power tracking of a wind energy system," Renewable Energy, 23, pp. 235-245.

[4] Mostafa, J., Ali , A., 2015, "Self-Tuning fuzzy PI-based controller of DFIG wind turbine for transient conditions enhancement," International Transactions on Electrical Energy Systems, 25, pp 2657–2673.

[5] Mohsen, D., Abolfazl, J., 2016, "Predictive control strategy to improve stability of DFIG-based wind generation connected to a large-scale power system," International Transactions on Electrical Energy Systems, Online Version of Record published before inclusion in an issue.

[6] Mahabuba, A., Abdullah , M., 2009, "Small signal stability enhancement of a multi-machine power system using robust and adaptive fuzzy neural network-based

power system stabilizer," International Transactions on Electrical Energy Systems, 19, pp. 978–1001.

[7] Utkin, V., 1993, "Sliding Mode Control Design Principles and Applications to Electric Drives," IEEE Trans on industrial electronics, 40.

[8] Patnaik, R., Dash, P., Mahapatra, K., 2016. "Adaptive terminal sliding mode power control of DFIG based wind energy conversion system for stability enhancement," International Transactions on Electrical Energy Systems, 26, pp. 750–782.

[9] Adjoudj, M., Abid, M., Aissaoui, A., Ramdani, Y., Bounoua, H., 2011, "Sliding mode control of doubly fed induction generator for wind energy turbine," Rev.Roum. Sci.Techn-Électrotechn. et Énerg,, 56, pp. 15-24.

[10] Benbouzid, M., Beltran, B., Amirat, Y., Yao, G., Han , J., 2014, "Second-order sliding mode control for DFIG-based wind turbines fault ride-through capability enhancement," ISA transactions, 53, pp. 827-833.

[11] PK, D., RK, P., 2014, "Adaptive second order sliding mode control of doubly fed induction generator in wind energy conversion system," Journal of Renewable and Sustainable Energy, 6(5), AIP Publishing.

[12] Wu, B., Lang, Y., Zargari, N., Kouro, S., 2011, "Power conversion and control of wind energy systems," John Wiley & Sons, Inc., United States of America.

[13] Poitiers, F., Bouaouiche, T., Machmoum, M., 2009, "Advanced control of a doubly-fed induction generator for wind energy conversion", Elect. Power Syst. Res., 79(7), pp. 1085–1096.

[14] Justo, J., Mwasilu, F., Jung, J.W., 2015, "Doubly-fed induction generator based wind turbines: A comprehensive review of fault ride-through strategies," Renewable and sustainable energy reviews, 45, pp. 447-467.

[15] Azar, A.T., 2016, "Advances and applications in sliding mode control systems," Q. Zhu (Ed.). Springer, 2016.

[16] Chiew Tsung, H., Zamberi, J., Ahmad Yusairi Bani, H., Lokman, A., Nur Aidawaty, R., 2017, " Design of super twisting algorithm for chattering suppression in machine tools," International Journal of Control, Automation and Systems, 3(15), pp. 1259-1266.

[17] Shtessel. Y., Plestan, F., Taleb, M., 2012, "A novel adaptive-gain supertwisting sliding mode controller," Methodology and application, Automatica, pp. 759–769.

[18] Jason J, Bonnie J. NWTC information portal (FAST V8). https://nwtc.nrel.gov/FAST8, 2015.